

Ab initio Calculations of Protonated Ethylenediamine-(water)₃ Complex: Roles of Intramolecular Hydrogen Bonding and Hydrogen Bond Cooperativity

Doo Wan Boo

Department of Chemistry, Yonsei University, Seoul 120-749, Korea

Received March 10, 2001

Ab initio density functional calculations on the structural isomers, the hydration energies, and the hydrogen bond many-body interactions for *gauche*-, *trans*-protonated ethylenediamine-(water)₃ complexes (*g*-enH⁺(H₂O)₃, *t*-enH⁺(H₂O)₃) have been performed. The structures and relative stabilities of three representative isomers (cyclic, tripod, open) between *g*-enH⁺(H₂O)₃ and *t*-enH⁺(H₂O)₃ are predicted to be quite different due to the strong interference between intramolecular hydrogen bonding and water hydrogen bond networks in *g*-enH⁺(H₂O)₃. Many-body analyses revealed that the combined repulsive relaxation energy and repulsive nonadditive interactions for the mono-cyclic tripod isomer, not the hydrogen bond cooperativity, are mainly responsible for the greater stability of the bi-cyclic isomer.

Keywords : Intramolecular hydrogen bonding, Hydrogen bond cooperativity, Relaxation energy, Nonadditive interactions.

Introduction

The solvation structure and dynamics of ions in water play an important role in many chemical and biological processes.^{1,2} The ion hydration processes in the first few solvation shells are of particular significance in determining the conformations and activities of biomolecules in water.^{3,4} The hydrogen bonding networks close to the ionic chromophores are generally governed by the competition between the ion-water and water-water interactions, different from those in the bulk where the water-water interactions are dominant. Furthermore, the ion-water interactions depend strongly on the structural and electronic nature of the central ions. In order to accurately describe the potential energy surfaces of hydrogen bond networks in the first few solvation shells where the continuum model^{5,6} fails to predict, it is inevitable to carry out the systematic studies on the hydration behaviors of various types of ions possessing different structural and electronic properties.

We have initiated combined experimental and *ab initio* theoretical studies of intramolecular hydrogen bond (IHB) containing protonated ion-(water)_n complexes to understand how the IHB in the protonated cores influences the hydrogen bond networks of the surrounding water molecules in the first and second solvation shells (referred to as 1^oH₂O and 2^oH₂O). We have previously reported the experimental and preliminary theoretical evidences for the IHB-assisted "bi-cyclic" structure of *gauche*-protonated ethylenediamine-(water)₃ complex (denoted as *g*-enH⁺(H₂O)₃ where *g*-enH⁺ = *gauche*-protonated ethylenediamine or *gauche*-NH₂CH₂CH₂-NH₃⁺) as a model study.⁷ We have shown in the communication that the hydration behavior of an IHB-containing protonated ion is quite different from the protonated ions that contain no IHBs due to strong interference between the IHB and the hydration bond networks. In this work, we describe the recent extended *ab initio* theoretical results on

the structures and hydration interactions of six representative isomers of *gauche*-, *trans*-protonated ethylenediamine-(water)₃ complex (*g*-, *t*-enH⁺(H₂O)₃), particularly focusing on the roles of the IHB and the hydrogen bond cooperativity.

Computational Details

The geometry optimizations and the vibrational frequency calculations for estimating zero-point energies (ZPE) of individual structural isomers have been performed at B3LYP/6-31+G(d) level using the GAUSSIAN-98 program.⁸ The total hydration energies and the contributions of many-body energy terms to the total hydration energies were evaluated at B3LYP level with various basis sets of 6-31+G(d), 6-31+G(d,p), 6-31++G(d,p), 6-311++G(d,p). The calculated energies were corrected for the ZPE and the basis set superposition errors (BSSE) estimated by the function counterpoise method.⁹

The decomposition of the total hydration energy ΔE_{hyd} for *g*-,*t*-enH⁺(H₂O)₃ was in this work performed following the works by Xantheas,¹⁰ Kim,¹¹ and Stillinger *et al.*¹² The total hydration energy ΔE_{hyd} for the 4-body complex (an enH⁺ core and three water molecules) can be written as the sum of the relaxation energy and the two-, three-, four-body energies as the following.

$$\begin{aligned} \Delta E_{hyd} &= E(1234) - \{E_{core} + 3E_W\} \\ &= \sum_{i=1}^4 E(i) - \{E_{core} + 3E_W\} \quad (\text{relaxation energy}) \\ &+ \sum_{i=1}^3 \sum_{j>i}^4 \Delta^2 E(ij) \quad (\text{two-body energy}) \\ &+ \sum_{i=1}^2 \sum_{j>i}^3 \sum_{k>j}^4 \Delta^3 E(ijk) \quad (\text{three-body energy}) \\ &+ \Delta^4 E(1234) \quad (\text{four-body energy}). \quad (1) \end{aligned}$$

where $E(i)$, $E(ij)$, $E(ijk)$, $E(1234)$ are the energies of the various monomers, dimers, trimers, and tetramer in the complex and E_{core} , E_W are the energies of isolated enH^+ ion and water molecules, respectively. The relaxation energy measures the extent of strains that drive the distortion of individual molecules in the complex. The pairwise additive two-body interaction energies and higher three-body and four-body nonadditive interaction energies are defined as the following equations.

$$\Delta^2 E(ij) = E(ij) - \{E(i) + E(j)\}, \quad (2)$$

$$\Delta^3 E(ijk) = E(ijk) - \{E(i) + E(j) + E(k)\} - \{\Delta^2 E(ij) + \Delta^2 E(ik) + \Delta^2 E(jk)\}, \quad (3)$$

$$\Delta^4 E(1234) = E(1234) - \{E(1) + E(2) + E(3) + E(4)\} - \{\Delta^2 E(12) + \Delta^2 E(13) + \Delta^2 E(14) + \Delta^2 E(23) + \Delta^2 E(24) + \Delta^2 E(34)\} - \{\Delta^3 E(123) + \Delta^3 E(124) + \Delta^3 E(134) + \Delta^3 E(234)\}. \quad (4)$$

The BSSE-corrected scheme has been used in this work to evaluate the contributions of many-body terms and relaxation energies in forming *g*-, *t*- $enH^+(H_2O)_3$ isomers. The BSSE-corrected energy of a subsystem (ijk) is evaluated in the full basis of a larger system (1234), and denoted by the term $E(ijk|1234)$. Accordingly, the n -body terms are substituted with the BSSE-corrected ones:

$$\Delta^2 \bar{E}(ij) = E(ij|1234) - \{E(i|1234) + E(j|1234)\}, \quad (5)$$

$$\Delta^3 \bar{E}(ijk) = E(ijk|1234) - \{E(i|1234) + E(j|1234) + E(k|1234)\} - \{\Delta^2 E(ij|1234) + \Delta^2 E(ik|1234) + \Delta^2 E(jk|1234)\}, \quad (6)$$

$$\Delta^4 \bar{E}(1234) = E(1234) - \{E(1|1234) + E(2|1234) + E(3|1234) + E(4|1234)\} - \{\Delta^2 E(12|1234) + \Delta^2 E(13|1234) + \Delta^2 E(14|1234) + \Delta^2 E(23|1234) + \Delta^2 E(24|1234) + \Delta^2 E(34|1234)\} - \{\Delta^3 E(123|1234) + \Delta^3 E(124|1234) + \Delta^3 E(134|1234) + \Delta^3 E(234|1234)\}. \quad (7)$$

Finally, the BSSE-corrected total hydration energy $\Delta \bar{E}_{hyd}$ is written as the sum of the relaxation energy and the BSSE-corrected two-body (2-B), three-body (3-B), and four-body (4-B) interaction energies as the following:

$$\Delta \bar{E}_{hyd} = E_R + \sum_{i=1}^3 \sum_{j>i}^4 \Delta^2 \bar{E}(ij) + \sum_{i=1}^2 \sum_{j>i}^3 \sum_{k>j}^4 \Delta^3 \bar{E}(ijk) + \Delta^4 \bar{E}(1234) \quad (8)$$

where E_R (relaxation energy) = $\sum_{i=1}^4 E(i) - \{E_{core} + 3E_W\}$.

Results and Discussion

Structures, energetics and hydration energies. Six representative minimum energy structures (cyclic, tripod, open) optimized at B3LYP/6-31+G(d), **I-III** for *g*- $enH^+(H_2O)_3$ and **IV-VI** for *t*- $enH^+(H_2O)_3$ are depicted in Figure 1 and their selected geometrical parameters listed in Table 1. They exhibit distinct inter- and intramolecular hydrogen bonding

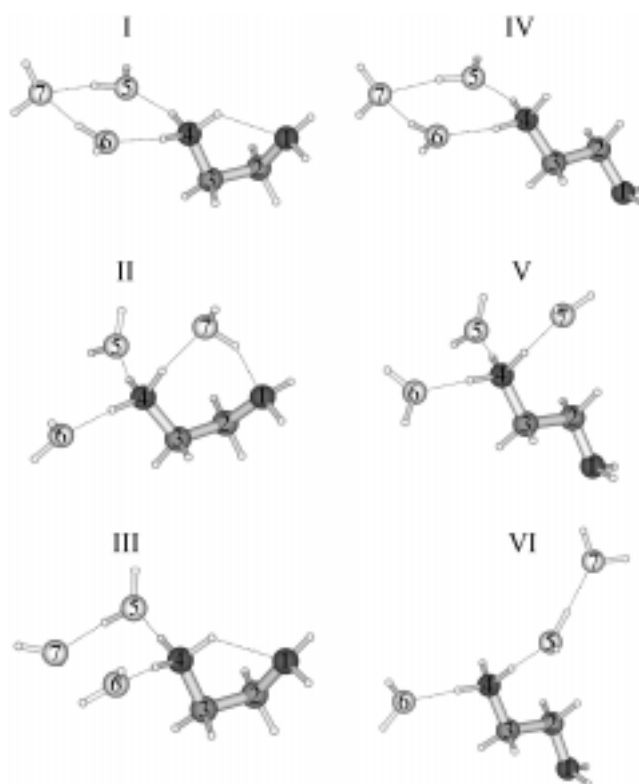


Figure 1. *Ab initio* optimized structural isomers **I-VI** of *g*-, *t*- $enH^+(H_2O)_3$ at B3LYP/6-31+G(d) level. They are named as bicyclic, mono-cyclic tripod, mono-cyclic open, mono-cyclic, non-cyclic tripod, and non-cyclic open isomers, respectively.

networks with three water molecules that are primarily bonded to the $-NH_3$ moieties of *g*-, *t*- enH^+ cores. Other structures with water molecules bonded to the $-NH_2$ and $-CH_2CH_2-$ moieties are predicted to be either unstable or substantially higher in energy. Table 2 illustrates the calculated electronic energies and the total hydration energies for these isomers (**I-VI**), and the zero-point energies (ZPE) and the BSSE corrections. The *gauche* isomers (**I-III**) are lower in energy by 6-7 kcal/mol than *trans*-isomers (**IV-VI**), somewhat reduced from the energy gap (~ 10 kcal/mol) between the isolated ions.

Isomers **I**, **IV** correspond to the characteristic cyclic solvated structures for *g*-, *t*- $enH^+(H_2O)_3$, named as “bicyclic” and “mono-cyclic” isomers, respectively. In these structures, the two $1^\circ H_2O$ molecules (5, 6) form charge-dipole bonds with two protons of the $-NH_3$ moieties, and the third $2^\circ H_2O$ molecule (7) acts as a double proton acceptor. The five-membered IHB ring structure of isomer **I** is somewhat distorted from that of isolated *g*- enH^+ ($\angle(N1-C2-C3-N4) = 49.3^\circ$ vs. 43°). As illustrated in Table 1, the cyclic hydrogen bond network in isomer **I** is less tightly bound than that in isomer **IV** evidenced by the slightly lengthened hydrogen bonds (R(O6-H4), R(O5-H4), R(O7-H5), R(O7-H6)) originating from the reduced charge densities in two protons of the $-NH_3$ moiety due to the IHB in the former (also see R(N4-Hⁱ4)). This result is consistent with the fact that the total hydration energy of isomer **IV** (-39.43 kcal/

Table 1. Selected geometric parameters for optimized structural isomers **I-VI**^a

	<i>gauche</i>			<i>trans</i>		
	I	II	III	IV	V	VI
R(N1-H ⁴) ^b	2.138	–	2.113	–	–	–
R(N1-H7)	–	1.885	–	–	–	–
R(N4-H ⁶) ^c	1.041	1.037	1.036	1.045	1.038	1.041
R(N4-H ⁴)	1.035	1.048	1.037	1.024	1.038	1.050
R(O6-H4)	1.791	1.838	1.835	1.762	1.833	1.807
R(O5-H4)	1.804	1.843	1.747	1.778	1.848	1.719
R(O5-H5)	0.980	0.971	0.987	0.980	0.971	0.988
R(O6-H6)	0.979	0.971	0.970	0.980	0.971	0.970
R(O7-H5)	1.930	–	1.781	1.925	–	1.769
R(O7-H6)	1.930	–	–	1.924	–	–
R(O7-H ⁴)	–	1.726	–	–	1.845	–
R(N4-O5)	2.805	2.872	2.787	2.786	2.884	2.770
R(N4-O6)	2.801	2.873	2.868	2.778	2.870	2.846
R(N4-O7)	4.314	2.742	4.867	4.309	2.880	4.822
R(O5-O7)	2.878	4.207	2.766	2.872	4.817	2.754
R(O6-O7)	2.874	4.839	6.166	2.867	4.591	6.869
R(O5-O6)	3.692	4.904	4.834	3.656	4.686	4.621
∠(H4-N4-H4)	105.40	108.55	109.71	104.55	107.71	107.28
∠(N1-H ⁴ -N4)	114.68	–	116.01	–	–	–
∠(N4-H ⁴ -O7)	–	161.87	–	–	175.67	–
∠(N4-H4-O5)	160.16	171.11	172.24	161.03	176.00	178.65
∠(N4-H4-O6)	162.44	175.05	173.84	163.14	177.14	176.94
∠(O5-H5-O7)	162.35	–	175.63	161.69	–	175.34
∠(O6-H6-O7)	161.06	124.46	–	160.72	–	–
∠(H5-O7-H6)	92.06	–	–	91.77	–	–
∠(N1-H7-O7)	–	150.75	–	–	–	–
∠(N1-C2-C3-N4)	49.31	72.39	49.40	-179.98	-179.23	179.67

^aGeometric parameters listed here are chosen only for directly bonded and hydrogen bonded atoms except for heavy atom distances. Distances are in Å and angles are in degrees. ^bH⁴ means intramolecular hydrogen bonded H atom among the hydrogen atoms bonded to heavy atom 4. ^cH⁶ means the hydrogen atom bonded to atom 4 and hydrogen-bonded to atom 6.

mol) is greater than that of isomer **I** (-36.21 kcal/mol) although the latter is ~6.6 kcal/mol more stable than the

former as mentioned previously (see Table 2).

Isomers **II**, **V** correspond to the tripod structures for *g*-, *t*-enH⁺(H₂O)₃ with the maximum strengths of ion-dipole interactions between -NH₃⁺ moiety and three H₂O molecules, and named as “mono-cyclic tripod” and “non-cyclic tripod” isomers, respectively. Of considerable importance is that the H₂O molecule bonded to the IHB proton penetrates into the five-membered IHB ring forming a seven-membered IHB-H₂O ring accompanied by a substantial change in the dihedral angle (∠(N1-C2-C3-N4)) from isolated *g*-enH⁺ (72.39° vs. 43°). Such water-bridged structure is known to be an important intermediate for facile proton transfer reactions in some protonated biomolecules.¹³⁻¹⁵ Consistent with the notion that the tripod structures are typically the most stable structures for R-NH₃⁺(H₂O)₃ complexes with no IHB due to the superior ion-dipole interactions,^{16,17} the tripod isomer **V** is calculated to be lowest in energy among three isomers of *t*-enH⁺(H₂O)₃ (**IV-VI**) when the ZPE and BSSE are corrected (Table 2). This trend of hydration, however, changes in the case of *g*-enH⁺(H₂O)₃ where the cyclic isomer **I** is ~1.2 kcal/mol more stable than the tripod isomer **II** due to the strong interference between IHB of *g*-enH⁺ core and water hydrogen bond networks. The origin for different hydration behaviors of *g*-enH⁺ core vs. *t*-enH⁺ core are further investigated in the subsequent part of this paper.

Isomers **III**, **VI** correspond to the “mono-cyclic open” and “non-cyclic open” structures being formed from simple bond rupture of one of the hydrogen bonds between 1°H₂O and 2°H₂O molecules from isomers **I**, **IV**. These loose isomers are thus expected to be favorable at high temperatures due to the large entropy contributions that lower the Gibbs free energies. Note that the open isomer **III** of *g*-enH⁺(H₂O)₃ is ~0.6 kcal/mol more stable than the tripod isomer **II**, different from the trend of *t*-enH⁺(H₂O)₃ due to the IHB-induced destabilization of the tripod isomer (**II**).

Although the energy differences among the cyclic, tripod, open isomers are small, the overall relative stabilities are in the orders of cyclic (**I**) > open (**III**) > tripod (**II**) for *g*-enH⁺(H₂O)₃ and tripod (**V**) > cyclic (**IV**) > open (**VI**) for *t*-enH⁺(H₂O)₃ when the ZPE BSSE are corrected (Table 2). The different hydration behaviors between *g*-enH⁺ and *t*-

Table 2. Electronic energies (E_{abs} , in hartree), and total hydration energies (ΔE_{hyd} , in kcal/mol) for structural isomers **I-VI** at B3LYP/6-31+G(d) level

	<i>gauche</i>			<i>trans</i>		
	I	II	III	IV	V	VI
E_{abs}	-420.2437	-420.2408	-420.2401	-420.2325	-420.2292	-420.2286
ZPE ^a	123.3159	122.6859	122.1346	122.8556	121.1447	121.6866
BSSE ^b	4.165	4.202	3.682	4.231	3.534	3.685
$E_{ZPE+BSSE}$	-420.0405 (0.0) ^c	-420.0386 (1.19)	-420.0396 (0.56)	-420.0300 (6.59)	-420.0305 (6.28)	-420.0288 (7.34)
ΔE_{hyd}	-46.81	-45.00	-44.59	-50.12	-48.06	-47.72
$\Delta E_{hyd+BSSE}$	-42.65	-40.80	-40.90	-45.89	-44.53	-44.04
$\Delta E_{hyd+ZPE+BSSE}$	-36.21	-34.99	-35.65	-39.43	-39.77	-38.74

^aZPE (Zero Point Energies) are calculated in kcal/mol using the scaled vibrational frequencies ($\times 0.98$). ^bBSSE (Basis Set Superposition Errors) are calculated in kcal/mol using counterpoise method (ref. 9). ^cNumbers in parentheses are the relative values with respect to structural isomer **I** (in kcal/mol).

Table 3. Total hydration energies (ΔE_{hyd} , in kcal/mol)^a at B3LYP level for structural isomers **I-VI** using various basis sets

	<i>gauche</i>			<i>trans</i>		
	I	II	III	IV	V	VI
6-31+G(d)	-42.65 (0.0) ^b	-40.80 (1.85)	-40.90 (1.75)	-45.89 (0.0)	-44.53 (1.36)	-44.04 (1.85)
6-31+G(d,p)	-42.25 (0.0)	-40.50 (1.75)	-40.71 (1.54)	-45.61 (0.0)	-44.33 (1.28)	-43.96 (1.65)
6-31++G(d,p)	-42.16 (0.0)	-40.45 (1.72)	-40.64 (1.52)	-45.50 (0.0)	-44.26 (1.24)	-43.88 (1.62)
6-311++G(d,p)	-42.07 (0.0)	-40.30 (1.77)	-40.65 (1.42)	-45.35 (0.0)	-44.37 (0.98)	-43.78 (1.57)

^aWith BSSE-corrected (in kcal/mol). ^bNumbers in parentheses are the relative values with respect to isomer **I** for *gauche* isomers and isomer **IV** for *trans* isomers (in kcal/mol).

Table 4. Many-body analysis of total hydration energies at B3LYP/6-31+G(d) and B3LYP/6-311++G(d,p) levels^a

	B3LYP/6-31+G(d)						B3LYP/6-311++G(d,p)					
	I	II	III	IV	V	VI	I	II	III	IV	V	VI
Two-body (2-B)												
M-W ₅	-15.38	-16.68	-16.20	-16.66	-17.23	-17.36	-15.40	-16.56	-16.27	-16.71	-17.16	-17.49
M-W ₆	-15.54	-17.10	-16.26	-16.97	-17.46	-17.60	-15.60	-17.10	-16.27	-17.05	-17.45	-17.60
M-W ₇	-6.78	-19.99	-5.62	-7.21	-17.03	-5.87	-6.58	-19.86	-5.44	-7.00	-16.99	-5.66
W ₅ -W ₆	2.00	0.68	0.88	2.06	0.83	0.88	1.91	0.64	0.83	1.97	0.79	0.84
W ₅ -W ₇	-4.04	0.39	-4.06	-4.01	0.84	-3.99	-3.94	0.38	-4.09	-3.92	0.79	-4.04
W ₆ -W ₇	-3.99	0.85	0.36	-3.97	0.86	0.31	-3.89	0.80	0.34	-3.87	0.81	0.28
$\Sigma M-W_n$ ^b	-37.70	-53.76	-38.08	-40.84	-51.72	-40.83	-37.57	-53.52	-37.98	-40.75	-51.60	-40.75
Sum (2-B)	-43.73	-51.84	-40.90	-46.76	-49.19	-43.64	-43.49	-51.70	-40.90	-46.57	-49.21	-43.67
Three-body (3-B)												
M-W ₅ -W ₆	1.89	1.46	1.63	2.11	1.43	1.75	1.92	1.47	1.64	2.15	1.45	1.78
M-W ₅ -W ₇	-1.77	1.07	-3.28	-1.89	1.40	-3.61	-1.79	1.08	-3.31	-1.90	1.41	-3.64
M-W ₆ -W ₇	-1.72	1.28	0.23	-1.87	1.40	0.27	-1.73	1.30	0.23	-1.88	1.41	0.27
W ₅ -W ₆ -W ₇	0.88	-0.05	0.14	0.90	-0.05	0.17	0.84	-0.05	0.13	0.86	-0.05	0.16
$\Sigma M-W_n-W_m$ ^b	-1.61	3.80	-1.43	-1.65	4.22	-1.59	-1.60	3.86	-1.44	-1.64	4.27	-1.59
Sum (3-B)	-0.73	3.75	-1.29	-0.75	4.17	-1.42	-0.76	3.81	-1.30	-0.77	4.22	-1.43
Four-body (4-B)												
Relaxation Energy	0.54	-0.08	0.15	0.60	-0.09	0.11	0.56	-0.09	0.16	0.61	-0.09	0.12
BE4	-42.65	-40.80	-40.90	-45.89	-44.53	-44.04	-42.07	-40.30	-40.65	-45.35	-44.37	-43.78
BSSE	4.16	4.20	3.68	4.23	3.53	3.68	3.00	3.10	2.81	3.03	2.73	2.83
Nonadditive Energy ^c	-0.19	3.67	-1.14	-0.15	4.08	-1.31	-0.20	3.72	-1.14	-0.16	4.13	-1.31

^aListed interaction energies are BSSE-corrected. ^bSum of ion-water interaction energies. ^cSum of 3-B and 4-B interaction energies

enH⁺ become more obvious when the sizes of basis sets are increased as shown in Table 3. With 6-311++G(d,p) basis set, for instance, the BSSE-corrected energy differences between the cyclic and tripod isomers of *g*-enH⁺(H₂O)₃ vs. *t*-enH⁺(H₂O)₃ (**I-II** vs. **IV-V**) further increased (1.77 vs. 0.98 kcal/mol), thus reinforcing the interference between IHB and intermolecular hydrogen bond interactions in *g*-enH⁺(H₂O)₃.

Many-body analyses. A quantitative account on the roles of IHB and hydrogen bond cooperativity on the hydration behavior of an IHB-containing protonated ion can be achieved by decomposing the total hydration energies of a system of *n*-bodies following many-body analysis scheme mentioned in Section II. The calculated many-body interaction energies for isomers **I-VI** at B3LYP/6-31+G(d) and B3LYP/6-311++G(d,p) levels are summarized in Table 4. The BSSE-corrected total hydration energies (denoted as BE4)

are divided into the BSSE-corrected 2-B, 3-B, 4-B and relaxation energies, and the sums of 2-B and 3-B ion-water interaction energies (denoted as $\Sigma M-W_n$ and $\Sigma M-W_n-W_m$) and the nonadditive interaction energies (3-B plus 4-B energies) are also listed. Since the predicted trends of many-body interactions at B3LYP/6-31+G(d) and B3LYP/6-311++G(d,p) are similar, so only the latter are discussed here.

For the pairwise additive 2-B terms, the $\Sigma M-W_n$ values for **I-VI** are -37.6, -53.5, -38.0, -40.8, -51.6, -40.8 kcal/mol, so the tripod isomers (**II, V**) are predicted to have greater ion-water interactions than the cyclic (**I, IV**) and open (**III, VI**) isomers by ~16 kcal/mol for *gauche* form (**II** vs. **I, III**) and ~11 kcal/mol for *trans* form (**V** vs. **IV, VI**). Of considerable interest is that the H₂O (7) molecule in isomer **II** participating in the seven-membered IHB ring has the greatest 2-B ion-water interaction energy (-19.86 kcal/mol). It is also noticeable that the H₂O (7) in isomers **I, III, IV, VI** having

no direct contact with the ion core still possesses ~6 kcal/mol attractive ion-water interaction energies. The water-water 2-B interaction energies (Sum (2-B) minus $\Sigma M-W_n$), on the other hand, are ~2 kcal/mol repulsive for the tripod isomers (**II**, **V**), ~6 kcal/mol attractive for the cyclic isomers (**I**, **IV**) with greater number of water-water hydrogen bonds, and ~3 kcal/mol attractive for open isomers (**III**, **VI**). The overall strength of pairwise additive 2-B interactions (Sum (2-B)) are in the order of **II** > **V** > **IV** > **VI** > **I** > **III** as illustrated in Table 4. Note that isomer **II** with smallest total hydration energy (BE4 = -40.3 kcal/mol) has the greatest 2-B interaction energy.

On the other hand, the sums of 3-B interaction energies are ~4 kcal/mol for the tripod isomers (**II**, **V**), ~ -0.8 kcal/mol for cyclic isomers (**I**, **IV**) and ~ -1.4 kcal/mol for open isomers (**III**, **VI**). These results are markedly different from the cases of neutral water clusters (H₂O)_n^{10,11} where the 3-B nonadditive interactions are quite attractive (e.g. ~ -6 kcal/mol for cyclic-(H₂O)₄ corresponding to ~25% of the total hydration energy), thus playing critical roles in forming cyclic structures. The repulsive 3-B interactions for the tripod isomers somewhat reduce their great stabilities gained from the superior 2-B interactions. Furthermore, the similar 3-B energies for the mono-cyclic tripod (**II**) and non-cyclic tripod (**V**) suggest that the 3-B terms are not responsible for the different hydration behavior of IHB-containing *g*-enH⁺ core vs. *t*-enH⁺ core.

A close examination of the data reveals that there are strong correlation between the signs of 3-B energies and hydrogen bond directionality (e.g. homodromic, heterodromic).¹¹ Extra stabilization of a particular hydrogen bonding network by many-body nonadditive interactions (known as hydrogen bond cooperativity) occurs only when the hydrogen bond networks are unidirectional or homodromic (e.g. donor-acceptor-donor-acceptor...). For instance, in isomer **I**, the 3-B terms for homodromic M-W₅-W₇, M-W₆-W₇ are attractive while those for bi-directional or heterodromic M-W₅-W₆, W₅-W₆-W₇ are repulsive. Among six isomers, the tripod isomers (**II**, **V**) with three heterodromic hydrogen bond networks (M-W₅-W₆, M-W₅-W₇, M-W₆-W₇) and one non-hydrogen bond network (W₅-W₆-W₇) possess the most repulsive 3-B interactions. To the contrary, the M-W₅-W₇ networks of the open isomers (**III**, **VI**) is the most attractive (-3.31, -3.64 kcal/mol) due to the less structural constraints in forming homodromic hydrogen bond networks. The fact that the 3-B nonadditive interactions in the first hydration shells of this particular ion slightly favor the open isomers than the cyclic isomers are also different from the cases of neutral chromophore-water clusters.¹⁸⁻²⁰

The 4-B interaction energies are negligible, so the overall nonadditive interaction energies (3-B + 4-B) are mostly determined by the 3-B terms consistent with the cases of neutral water clusters.^{10,11} A remarkable difference in energy among six isomers is found in the relaxation energies that measure the degree of distortion in individual molecules in each isomer. The relaxation energy of isomer **II** is 7.7 kcal/mol, considerably larger than those of other isomers (0.7-1.6

kcal/mol). The larger relaxation energy for isomer **II** can be attributed to the large geometrical changes in *g*-enH⁺ core and H₂O (7) participating in the seven-membered ring network (also see Table 1). The large increase in the dihedral angle of *g*-enH⁺ backbone (\angle (N1-C2-C3-N4) = 72.4°) from free *g*-enH⁺ (43°) is worthy to be noticed. Consequently, the large relaxation energy of the mono-cyclic tripod isomer (**II**) arising from strong interference between IHB and water hydrogen bond networks is mainly responsible for the different hydration behaviors of *g*-enH⁺ vs. *t*-enH⁺.

The overall stabilities of hydrated structures are determined ultimately by the competition between pairwise additive 2-B terms, nonadditive terms, and relaxation energies. The results of many-body analyses suggest that the hydrogen bond cooperativity (or attractive nonadditive interactions) does not play an important role; instead, the combined repulsive relaxation energy and repulsive nonadditive interactions of the competing mono-cyclic tripod isomer (**II**) are responsible for the preferential formation of bi-cyclic isomer (**I**). The strong interactions between IHB and water hydrogen bond networks for *g*-enH⁺ core change the entire landscape of hydrogen bond many-body interactions from those of non-IHB protonated ions.

Conclusions

In this work, we describe the extended *ab initio* theoretical results on the structural isomers and hydration energies, and their many-body interactions in the cases of *gauche*-, *trans*-protonated ethylenediamine-(water)₃ complexes. We show that the structures and relative stabilities of three representative isomers (cyclic, tripod, open) between *g*-enH⁺(H₂O)₃ and *t*-enH⁺(H₂O)₃ are quite different due to strong interference between IHB and water hydrogen bond networks. Many-body analyses reveal that the strong IHB-water interactions result in the large relaxation energies, and the combined repulsive relaxation energy and repulsive nonadditive interactions for the mono-cyclic tripod isomer (**II**), not the hydrogen bond cooperativity, are mainly responsible for the preferential formation of bi-cyclic isomer (**I**).

Acknowledgment. This work was financially supported by Korea Research Foundation Grant (KRF-2000-042-D00036), Korea. The author acknowledges the computing time allocations for the SGI Origin-2000 workstation by Department of Mathematics, Yonsei University, Korea.

References

- (a) Tarek, M.; Tobias, D. J. *J. Am. Chem. Soc.* **1999**, *121*, 9740. (b) Kim, K. S. *et al. Proc. Natl. Acad. Sci. USA*, **2000**, *97*, 6373. (c) Cleland, W. W.; Kreevoy, M. M. *Science* **1994**, *264*, 1887. (d) Creighton, T. E. *Proteins: Structure and Molecular Properties*; Freeman: New York, 1993.
- (a) Woenckhaus, J.; Hudgins, R. R.; Jarrold, M. F. *J. Am. Chem. Soc.* **1997**, *119*, 9586. (b) Marx, D. M.; Tuckerman, M. E.; Hutter, J.; Parrinello, M. *Nature* **1999**, *397*, 601. (c) Kim, K. S. *et al. Chem. Rev.* **2000**, *100*, 4145.

3. (a) Mao, Y.; Ratner, M. A.; Jarrold, M. F. *J. Am. Chem. Soc.* **2000**, *122*, 2950. (b) Hill, R. B.; Hong, J.; DeGrado, W. F. *J. Am. Chem. Soc.* **2000**, *122*, 746. (c) Choi, H. S. *et al. Proc. Natl. Acad. Sci. USA*, **1998**, *95*, 12094.
 4. (a) Jarrold, M. *Acc. Chem. Res.* **1999**, *32*, 360. (b) Clary, D. C.; Benoit, D. M.; Mourik, T. V. *Acc. Chem. Res.* **2000**, *33*, 441.
 5. Bandyopadhyay, P.; Gordon, M. S. *J. Chem. Phys.* **2000**, *113*, 1104.
 6. Tomasi, J.; Perisco, M. *Chem Rev.* **1994**, *94*, 2027.
 7. Boo, D. W.; Chang, H. C.; Lee, Y. T. *J. Phys. Chem. A* (submitted).
 8. Frisch, M. J. *et al. GAUSSIAN 98*; Gaussian, Inc.: Pittsburgh, Pennsylvania, 1998.
 9. Boys, S. F.; Bernardi, F. *Mol. Phys.* **1970**, *19*, 553.
 10. Xantheas, S.S. *J. Chem. Phys.* **1994**, *100*, 7523. Xantheas, S.S. *Chem. Phys.* **2000**, *258*, 225.
 11. (a) Kim, K. S. *et al. Chem. Phys. Lett.* **1986**, *131*, 451. (b) Mhin, B. J. *et al. J. Chem. Phys.* **1994**, *100*, 4484. (c) Kim, K. S. *et al. J. Chem. Phys.* **1995**, *102*, 839. (d) Baik, J. *et al. J. Chem. Phys.* **1999**, *110*, 9116.
 12. Hankins, D.; Moskowitz, J. W.; Stillinger, F. H. *J. Chem. Phys.* **1970**, *53*, 4544.
 13. Green, M. K.; Lebrilla, C. B. *Int. J. Mass Spectrom. Ion Proc.* **1998**, *175*, 15.
 14. Sinnige, C. G.; de Koning, L. J.; Nibbering, N. M. M. *Int. J. Mass Spectrom.* **2000**, *195*, 115.
 15. Smedarchina, Z.; Siebrand, W.; Fernandez-Ramos, A.; Gorb, L.; Leszczynski, J. *J. Chem. Phys.* **2000**, *112*, 566.
 16. Jiang, J. C.; Chang, H. C.; Lee, Y. T.; Lin, S. H. *J. Phys. Chem. A* **1999**, *103*, 3123.
 17. Wang, Y. S.; Chang, H. C.; Jiang, J. C.; Lin, S. H.; Lee, Y. T.; Chang, H. C. *J. Am. Chem. Soc.* **1998**, *120*, 8777.
 18. Frost, R. K.; Hagemester, F. C.; Arrington, C. A.; Schleppenbach, D.; Zwier, T. *J. Chem. Phys.* **1996**, *105*, 2605.
 19. Florio, G. M.; Gruenloh, C. J.; Quimpo, R. C.; Zwier, T. S. *J. Chem. Phys.* **2000**, *113*, 11143.
 20. Mitsuzuka, A.; Fujii, A.; Ebata, T.; Mikami, N. *J. Chem. Phys.* **1996**, *105*, 2618.
-